Journal of the European Ceramic Society 22 (2002) 2517–2525

www.elsevier.com/locate/jeurceramsoc

Effect of heat treatments on microstructure and creep behaviour of silicon nitride based ceramics

Andreas Rendtel[a,*], Heinz Hübner[b]

[a]GKSS Research Center, Institute for Materials Research, Max-Planck-Straße, D-21502 Geesthacht, Germany
[b]Technical University Hamburg-Harburg, Materials Science and Technology Group, D-21071 Hamburg, Germany

Received 4 December 2001; accepted 17 April 2002

Abstract

Silicon nitride based ceramics were exposed to reducing and/or oxidising atmospheres and subsequently creep-tested in uniaxial tension. The microstructure was examined before and after creep testing. All post-densification treatments caused grain growth. Additionally, treatments in nitrogen atmosphere lead to a reduction of the total oxygen content. Grain coarsening and reduction of the oxygen content were less pronounced for materials containing submicron-sized silicon carbide particles. The creep rates at 1500 °C of materials heat-treated in nitrogen atmosphere were found to be reduced by up to about one order of magnitude. The reduction, however, was only partially due to grain growth. As an additional effect, modifications of the grain-boundary structure were identified. Furthermore, the treatments caused an increase in the activation energy for creep leading to a more pronounced reduction of the creep rate at lower temperatures. Oxidised materials showed only minor changes of the creep resistance. Chemical modifications of the intergranular phase, grain growth, and a pronounced interlocking of the grain facets in the vicinity of SiC particles are suggested to explain the increased creep resistance of the Si_3N_4/SiC nanocomposites, the latter two phenomena being considered to have the largest effects on the creep resistance.

Keywords: Creep behaviour; Grain growth; Microstructure; Nanocomposites; Silicon nitride; Thermal treatment

1. Introduction

Silicon nitride (Si_3N_4) and its composites are promising materials for high-temperature applications. Many efforts have been made in the past to increase high-temperature strength, creep and oxidation resistance, and lifetimes of such Si_3N_4-based ceramics. Different microstructural design concepts were pursued to improve the mechanical properties at elevated temperatures—a short overview is given in Ref. 1. Best results were obtained so far by the nanocomposite concept proposed by Niihara.[2] However, to achieve materials of outstanding creep resistance several microstructural design approaches, i.e. careful control of the type and amount of the densification additive, incorporation of nano/submicron-sized SiC particles, adjustment of a specific Si_3N_4 grain size during densification, and a thermal treatment of the densified material, have to be applied in combination.[1] But, the basic effects of the added SiC particles and of the thermal treatments are not fully understood up to now.

Three possible influences of the SiC particles are discussed: *microstructural*, *micromechanical*, and *chemical* effects.[3] In this context *microstructural* effect means the modification of grain size and shape by the presence of the SiC particles. The *micromechanical* effect can be summarised as inhibition of grain-boundary sliding by grain pinning, and *chemical* influences consist in the reduction of the oxygen content of the intergranular phase leading to a higher viscosity.

It was the purpose of the present study to investigate the effects of thermal treatments on microstructure and creep behaviour of Si_3N_4 and Si_3N_4/SiC nanocomposite ceramics. It was proved whether incorporated SiC particles affect the oxygen content and if such an effect can be substituted by a thermal treatment in a reducing environment. Therefore, specimens of a monolithic Si_3N_4 and a Si_3N_4/SiC nanocomposite were subjected to different heat treatments. Their microstructure and creep

* Corresponding author. Present address: Wacker-Chemie GmbH, Max-Schaidhauf-Str. 25, D-87437 Kempten, Germany. Tel.: +49-831-5618-457; fax: +49-831-5618-8457.
E-mail address: andreas.rendtel@wacker.com (A. Rendtel).

0955-2219/02/$ - see front matter
PII: S0955-2219(02)00112-7

behaviour was investigated before and after the treatments to separate the various effects mentioned before.

2. Experimental details

The silicon nitride based ceramics tested in this study were fabricated at the Fraunhofer Institute IKTS, Dresden, Germany. The main constituent was a commercial high purity α-Si_3N_4 powder (SN E-10, Ube Industries, Yamaguchi, Japan). Y_2O_3 (grade fine, H.C. Starck, Goslar, Germany) was applied as a densification aid. To produce a Si_3N_4/SiC nanocomposite an amorphous SiCN powder[4] (~80% SiC; Institute of Inorganic Chemistry, Academy of Science of Latvia, Riga, Latvia) was added. Homogeneous mixtures of the starting powders were obtained by milling in isopropanol in a planetary mill. After drying and calcinating at 450 °C for 1 h, the powder mixtures were densified by hot-pressing (HP) for 1 h under a pressure of 30 MPa in nitrogen atmosphere. Further details of the fabrication process were described elsewhere.[5] The composition of the materials and their designations are given in Table 1. To achieve materials of comparable grain size after HP the monolithic Si_3N_4–8Y– was densified at 1805 °C and the Si_3N_4/SiC nanocomposite—8YH10SCp—at 1840 °C.

Thermal treatments of hot-pressed materials were performed at 1700 °C in a high purity nitrogen atmosphere, i.e. a reducing environment with a very low oxygen partial pressure, for 4 and 9 h (designations T4 and T9, respectively) and at 1500 °C in air atmosphere, a oxidising environment with a high oxygen partial pressure, for 200 h (designation ox). All material designations are summarised in Table 1.

Creep testing was performed on hot-gripped, four-pin loaded, dog-bone shaped tensile specimens of 56 mm total length with a gage cross-section of 2×4.6 mm. The specimens were cut from the hot-pressed billets and ground with a diamond wheel (grain size 46 μm). Selected specimens were heat-treated as described above. After treatment the flat specimen surfaces were ground again to remove a layer of about 100–150 μm. The as-ground specimens were tested in air atmosphere under constant load (100 MPa) and temperature in the range 1500–1600 °C in a screw-driven universal testing machine. Flag-based scanning laser extensometry (laser extensometer LE45HT0.2, Fiedler Optoelektronik GmbH, Lützen, Germany) was used to continuously measure the specimen elongation. Details of the tensile creep facility are described elsewhere.[6] Since creep tests were performed in air atmosphere they represent also thermal treatments in a oxidising environment.

From the elongation data, the true creep strain, ε, was calculated as a function of time, t. The creep rate, $\dot{\varepsilon}$, was calculated from the slope of the ε *vs.* t curve. The Norton equation:[7]

$$\dot{\varepsilon}_s = A \cdot \sigma^n \cdot \frac{1}{d^m} \cdot \exp\left(-\frac{Q_c}{RT}\right) \quad (1)$$

was used to describe the steady-state creep rate, $\dot{\varepsilon}_s$. In Eq. (1), A is a microstructure dependent constant, σ is the stress, n is the stress exponent, d is the grain size, m is the grain-size exponent, Q_c is the activation energy for creep, and T and R have their usual meaning. The parameter Q_c was determined from steady-state strain-rate ratios of temperature jump tests.

Microstructural characterisation of hot-pressed, heat-treated, and creep-tested materials was done on commercial scanning and transmission electron microscopes (SEM: Gemini 1530, LEO Elektronenmikroskopie GmbH, Oberkochen, Germany; TEM: CM-20, Philips Electronic Instruments, Eindhoven, the Netherlands). SEM observations were performed on polished and plasma-etched sections covered with a thin layer of gold to avoid charging. Samples for the TEM investigations (TEM investigations were performed at the University Bayreuth, Germany, together with Professor H.-J. Kleebe, who is now with the Colorado School of Mines, Golden, CO, USA). were prepared by the usual procedures for ceramics, i.e. slicing, disc cutting, mechanical grinding/polishing, dimpling, and ion milling. A thin layer of carbon was deposited on the thin foil to avoid charging in the TEM.

The calliper dimension, which is defined as the minimum diameter of an object, of more than 1000 grains per material was measured on SEM micrographs to determine the size distribution. Taking the measured

Table 1
Composition and treatments of the materials studied and their designations

Composition (wt.%)	Treatment[a]			
	Oxidation	HP	T4	T9
8 Y_2O_3 + 92 Si_3N_4	No	8Y	8YT4	8YT9
	Yes	8Yox	8YT4ox	8YT9ox
8 Y_2O_3 + 10 SiC + 82 Si_3N_4	No	8YH10SCp	8YH10SCpT4	8YH10SCpT9
	Yes	8YH10SCpox	8YH10SCpT4ox	8YH10SCpT9ox

[a] For treatment conditions see text.

diameters, d_i, the mean grain size, d_m, was calculated according to

$$d_m = \frac{1}{n}\sum_{i=1}^{n} d_i \quad (2)$$

with n = number of grains.

The phase composition of the materials was analysed by X-ray diffraction (XRD) using CuK_α-radiation. The total oxygen content of the bulk materials was measured by a commercial hot-gas extraction analyser (Model TC-436, LECO Co., St. Joseph, MI, USA) according to DIN ISO 4491, Part 4 (measurements were performed at the Fraunhofer Institute IKTS, Dresden, Germany). Three measurements of the oxygen content were performed for each sample.

3. Results

3.1. Microstructure

Typical microstructures of hot-pressed and heat-treated monolithic Si_3N_4 and Si_3N_4/SiC nanocomposites are shown in Figs. 1 and 2, respectively. In general, the materials consist of elongated and small globular Si_3N_4 grains with random orientation and a grain-boundary phase concentrated to a large extent in multigrain junctions. The nanocomposites additionally contain globular nano- and submicron-sized SiC particles mainly located in between the Si_3N_4 grains. Part of the SiC particles, in particular those smaller than 100–150 nm, are found within larger Si_3N_4 grains. The size distributions of the Si_3N_4 grains as well as of the SiC particles are rather broad and cover a range starting from about 20 nm up to approximately 1.5 μm. For the nanocomposites no difference could be found between the size distribution of the Si_3N_4 grains and that of the SiC particles. Hence, each nanocomposite was characterised by a single size distribution including the data of the Si_3N_4 and the SiC grains. Examples of grain-size distributions are plotted in the form of sum frequency vs. grain size in Fig. 3 for those materials, the microstructure of which is shown in Figs. 1 and 2. The data can be approximated by log-normal distributions which are represented by the straight lines in Fig. 3.

It can easily be recognised that the treatment T9 caused substantial grain growth in the monolithic material, but only minor grain coarsening in the

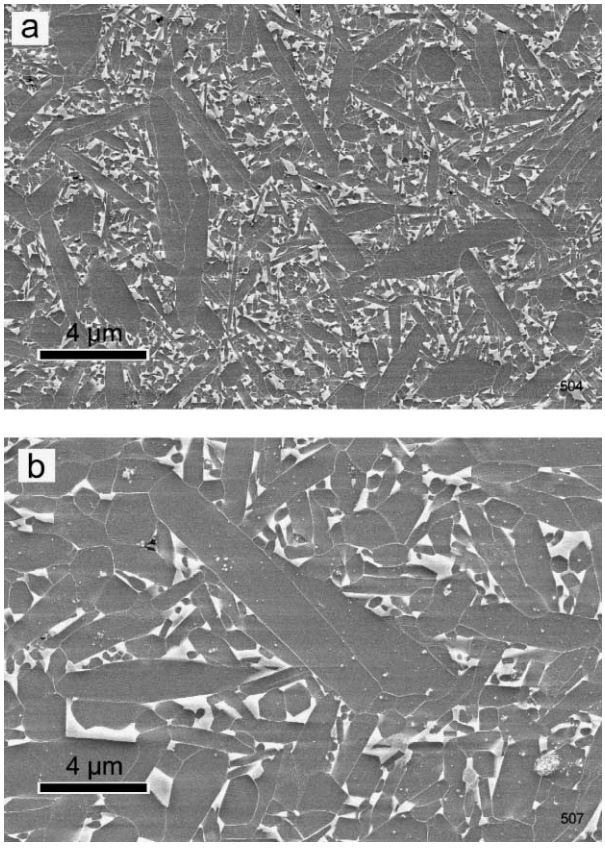

Fig. 1. Microstucture of materials 8Y (a) and 8YT9 (b) after creep tests c1 and c3, respectively (for creep conditions see Table 2 and Fig. 5; dark: Si_3N_4 grains, bright: secondary phase).

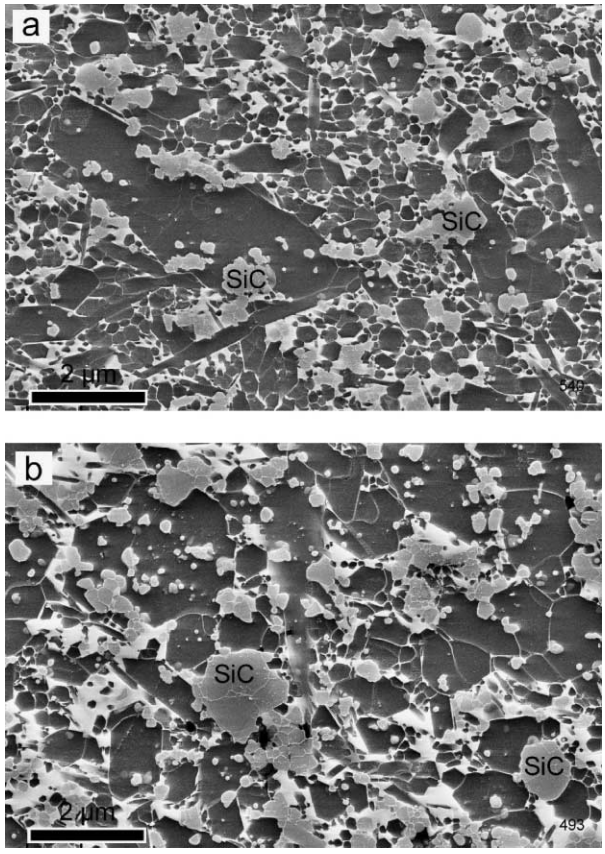

Fig. 2. Microstucture of the as-processed materials 8YH10SCp (a) and 8YH10SCpT9 (b) (dark: Si_3N_4 grains, bright: secondary phase, grey: SiC).

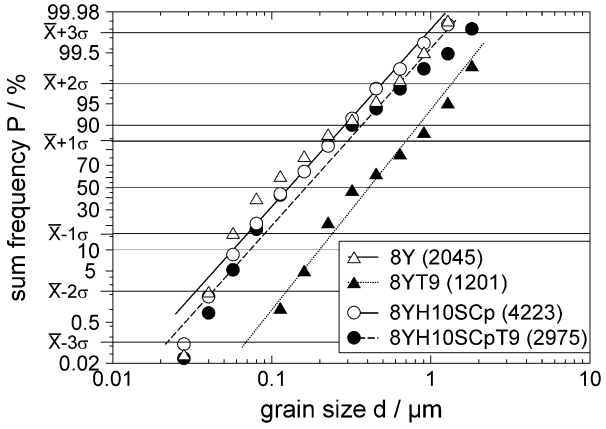

Fig. 3. Grain-size distributions of the as-processed materials 8Y, 8YT9, 8YH10SCp, and 8YH10SCpT9. The number of grains counted is given in the parentheses.

nanocomposite. Comparison of the grain-size distributions of both material groups reveals that the shape of the distribution is nearly not affected. For all grain-size distributions measured in this study the mean grain size, d_m, was calculated according to Eq. (2). Please note that d_m is not the same as the median grain size, d_{50}, that can be taken from Fig. 3 at 50% sum frequency. The obtained values of d_m are shown in Fig. 4. It can be seen that all heat-treatments (T4, T9, creep tests) caused grain growth. The mean grain size of the monolithic Si_3N_4 grew up to five times (HP→T9 + c3). Largest contributions to grain growth were obtained for the treatments T4 and T9. Grain coarsening during creep tests very much depended on temperature and test duration (see Table 2 and compare with Fig. 4). For all kinds of heat treatments, grain growth was much less pronounced in the nanocomposite than in the monolithic specimens. The maximum grain coarsening in the nanocomposite

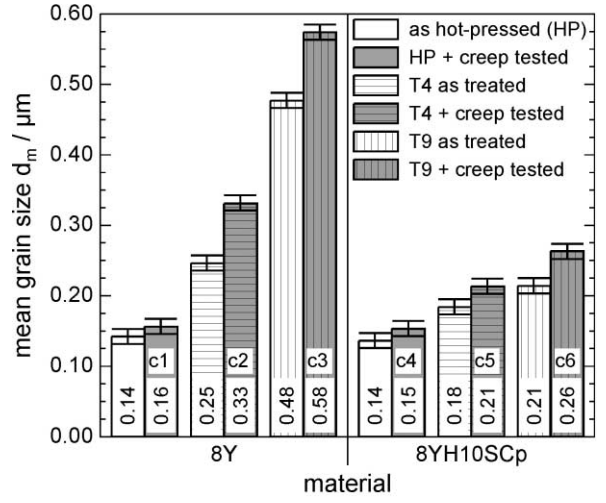

Fig. 4. Mean grain size of materials 8Y and 8YH10SCp after different treatments (for temperature conditions of creep tests c1…c6 see Table 2).

Table 2
Temperatures and test duration (h) for creep tests c1…c6

Material	Test	1500 °C	1525 °C	1550 °C	1575 °C	1600 °C
8Y	c1	25	5	2	0.5	0.35
8YT4	c2	106.5	28	3	–	–
8YT9	c3	162	53	15	–	–
8YH10SCp	c4	40	5.5	1.8	1	0.1
8YH10SCpT4	c5	135	35	22	8	0.2
8YH10SCpT9	c6	344	118	7.5	–	–

only reached a factor smaller than two (crept specimen 8YH10SCpT9-c6).

The phase composition of silicon nitride ceramics is another important feature thought to largely affect the high-temperature properties. The main phases of the hot-pressed materials were β-Si_3N_4 and small amounts of α-Si_3N_4. The nanocomposite additionally contained α-SiC. In the monolithic Si_3N_4 both N-apatite (H-phase, $Y_5N(SiO_4)_3$, 26.1 wt.% oxygen) and N-wollastonite (K-phase, $YSiO_2N$, 19.6 wt.% oxygen) were detected as crystalline grain-boundary phases. Thus, compared with N-wollastonite, N-apatite is the oxygen-rich phase. However, in the nanocomposite only N-wollastonite was found as crystalline grain-boundary phase. The various treatments caused different changes in the phase composition of the bulk materials.

Treatments of the monolithic Si_3N_4 in a reducing environment (T4 and T9) shifted the composition of the intergranular phase from N-apatite-rich to N-wollastonite-rich. Furthermore, the α-Si_3N_4 present after densification (HP) was completely transformed to β-Si_3N_4. In the nanocomposite, changes of the grain-boundary phase composition could not be detected. But, transformation of α-Si_3N_4 to β-Si_3N_4 occurred and was completed in material 8YH10SCpT9. Treatments in a oxidising environment (ox, creep tests) changed the grain-boundary phase composition of all materials completely to N-apatite, even that of material 8YH10SCpT9ox. Furthermore, these treatments caused the small amounts of α-Si_3N_4 to be transformed to β-Si_3N_4.

The treatments in reducing and oxidising atmospheres also affected the total oxygen content of the bulk materials. The results of the oxygen content measurements are summarised in Table 3. The "theoretical" oxygen content (calculated from the composition of the starting powders—see Table 1 in Ref. 5) of the materials 8Y and 8YH10SCp is 2.99 and 2.82 wt%, respectively. Compared to these values the measured oxygen content of the hot-pressed materials is lower by about 5% in 8Y and 10% in 8YH10SCp. The treatments T4 and T9 lead to a further reduction of the oxygen content by about 12 and 24% in 8YT4 and 8YT9, respectively, and about 2.4% in 8YH10SCpT4. Due to oxidation the oxygen content of the bulk of all materials increased to some

Table 3
Total oxygen content (wt.%) of bulk materials after different treatments

Material	Treatment	HP	T4	T9
8Y	As processed	2.84	2.50	2.17
	after subsequent oxidation	2.86	2.68	2.23
8YH10SCp	As processed	2.54	2.48	n.d.[a]
	after subsequent oxidation	2.66	2.66	n.d.[a]

[a] Not determined.

extent. For materials 8YT4ox and 8YT9ox the oxygen pick up was much smaller than the oxygen release during the treatments T4 and T9.

3.2. Creep behaviour

Typical creep curves (strain vs. time) obtained for temperature jump tests in uniaxial tension at 100 MPa are shown in Fig. 5. The creep behaviour of all materials (including the heat treated ones) is characterised by a primary creep range and pronounced steady-state creep. A tertiary creep regime was not observed. Comparing the creep curves at 1500 °C (first part of each curve) reveals that material 8YH10SCp deforms less than material 8Y and that the creep rates of the heat-treated materials (T9) are much smaller than those of the hot-pressed materials.

The effect of treatments in a reducing environment on the temperature dependence of the steady-state tensile creep rate of the monolithic Si_3N_4 and the nanocomposite is shown in Fig. 6. The treatments resulted in reduced creep rates. In Table 4 are given creep-rate ratios (CRR) calculated according to

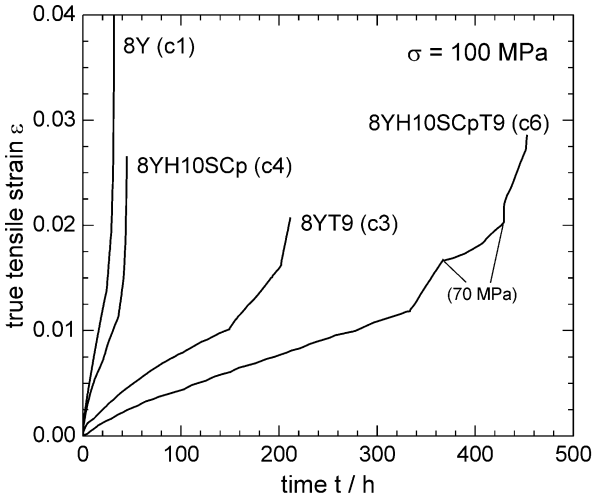

Fig. 5. Strain vs. time curves of materials 8Y, 8YT9, 8YH10SCp, and 8YH10SCpT9 obtained in temperature jump tests at 100 MPa (first temperature is 1500 °C, further temperatures and durations of tests c1…c6 see Table 2).

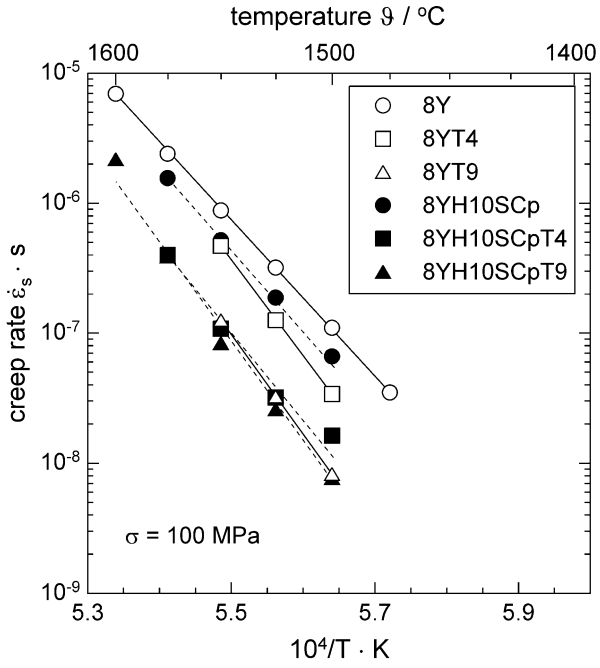

Fig. 6. Effect of heat treatments in nitrogen atmosphere on the temperature dependence of the steady-state tensile creep rate at 100 MPa (creep rate data as measured).

$$\text{CRR-T4} = \frac{\dot{\varepsilon}_s^{T4}}{\dot{\varepsilon}_s^{HP}} \quad \text{and} \quad \text{CRR-T9} = \frac{\dot{\varepsilon}_s^{T9}}{\dot{\varepsilon}_s^{HP}}. \tag{3}$$

The smallest CRR of 0.075 and, hence the largest effect of the thermal treatment was obtained for material 8YT9. Additionally, the treatments caused a distinct rise in the activation energy for creep, Q_c, from 1140 kJ/mol (for HP materials) up to 1420 kJ/mol (for T9 materials).

The effect of the oxidation treatment on the temperature dependence of the steady-state tensile creep rate of the nanocomposite is shown in Fig. 7. Creep rate data plotted in this figure are corrected for a mean grain size of $d_m = 0.15$ μm. The correction procedure is described below. It becomes obvious that the creep behaviour of neither material 8YH10SCp nor of material 8YH10SCpT9 is affected by the oxidation. This result seems to be contrary to that found in Ref. 8. However, in this earlier investigation the specimens were oxidised for 1000 h prior to testing, resulting in more pronounced changes of the microstructure.[9] Additionally, grain growth was not considered for the interpretation of the results. So, it can be stated that only severe oxidation affects the creep resistance of the materials of this study.

4. Discussion

In the following paragraphs, an attempt is made to improve the understanding of the role of SiC particles in Si_3N_4/SiC nanocomposites. As proposed previously,[3]

Table 4
Effect of heat treatments T4 and T9 on the creep rate $\dot{\varepsilon}_s$ at 1500 °C/100 MPa (data taken from Fig. 6) and on grain size d_m

	T4			T9		
Material	CRR-T4[a]	GSR-T4[b]	CRR-T4$_{corr.}$[c]	CRR-T9[a]	GSR-T9[b]	CRR-T9$_{corr.}$[c]
8Y	0.31	2.1	0.65	0.075	3.7	0.28
8YH10SCp	0.25	1.4	0.34	0.12	1.7	0.20

[a] Creep-rate ratio calculated according to Eq. (3).
[b] Grain-size ratio.
[c] Creep-rate ratio corrected for $d_m = 0.15$ μm using Eq. (5).

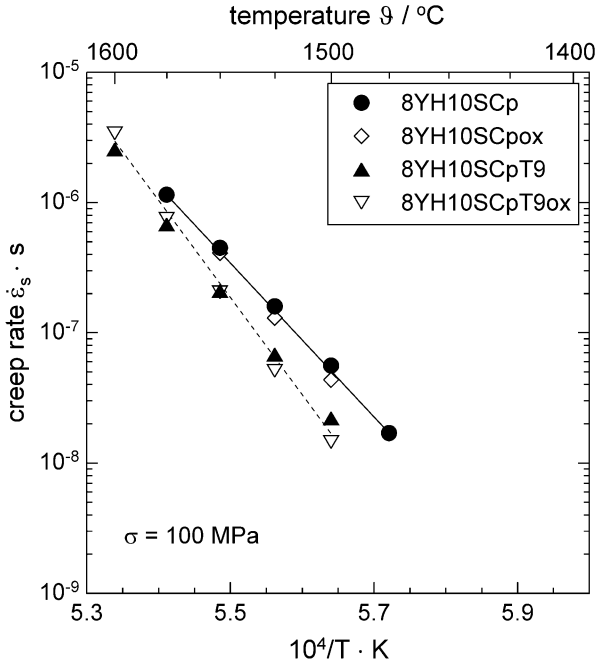

Fig. 7. Effect of oxidation treatment on the temperature dependence of the steady-state tensile creep rate at 100 MPa (creep rate data corrected for $d_m = 0.15$ μm).

three types of influences can be expected to cause improvements of the high-temperature properties, i.e. *microstructural*, *micromechanical*, and *chemical* effects. However, a deterioration of properties may be found as well. It was argued by Niihara[2] that the inhibition of grain-boundary sliding by SiC particles located at matrix grain boundaries, i.e. a *micromechanical* effect, is responsible for the improved creep resistance of nanocomposites. This suggestion, however, has been verified up to now only for Al_2O_3/SiC nanocomposites by Ohji et al.[10] In a TEM study they found evidence of grain pinning by a small SiC particle located on the alumina grain boundary. Moreover, the improvement in creep resistance of Si_3N_4/SiC nanocomposites is much smaller than that found in Al_2O_3/SiC nanocomposites.[3,11]

In recent publications[1,3] we suggested that the most likely influence of the SiC particles in Si_3N_4/SiC nanocomposites is a chemical interaction rather than a micromechanical effect. It was assumed that this *chemical* effect consists of a reaction between SiC and amorphous silica, resulting in a reduction of the amount of intergranular amorphous silica remnants, thereby increasing the grain-boundary viscosity η and, hence, the creep resistance. If this explanation is true, a variation of the oxygen content between monolithic and SiC containing Si_3N_4 should be detectable. Such a modification of the grain-boundary chemistry would also affect the diffusion coefficient D of matrix material along the grain boundary and the properties at the Si_3N_4/glass interface, i.e. the interfacial energy γ_I. Furthermore, if the improvement of the creep resistance is mainly due to a reduced silica content at the Si_3N_4 boundaries, it seems likely that such improvement can equally be achieved by suitable heat treatments in a reducing environment of monolithic Si_3N_4 that does not contain any SiC. Additionally, the question arises if this effect is reversible so that it can be inverted by a subsequent oxidation treatment. To find answers to these questions a monolithic Si_3N_4 material and an Si_3N_4/SiC nanocomposite were heat-treated as described in this work. The results are discussed in terms of the arguments mentioned before.

As shown in Table 3, the oxygen content of hot-pressed Si_3N_4 in the as-received state is lowered by 11% due to a 10% SiC addition (compare materials 8Y and 8YH10SCp), whereas the reducing heat treatments T4 and T9 cause a reduction of the oxygen content of hot-pressed Si_3N_4 by 12 and 24%, respectively. These results confirm that the SiC dispersion reacts with oxygen-containing phases resulting in a decline of the oxygen content and that an even more pronounced reduction of the oxygen content can be obtained by a heat treatment in a reducing environment. This is evidence that the oxygen depletion achieved by an SiC dispersion can be substituted by a reducing heat treatment. Oxygen pickup during a subsequent oxidation treatment is only small, demonstrating that the oxygen depletion is not reversible. The consequences for the creep resistance will be discussed later.

The various heat treatments were also accompanied by changes in the phase composition, in particular of the intergranular phases. The presence of the oxygen-rich N-apatite and of the comparably oxygen-poor N-wollastonite correlates well with the total oxygen content. Materials with a markedly reduced oxygen content

such as 8YH10SCp and the N_2-treated materials 8YT4 and 8YT9 were found to contain higher amounts of the oxygen-poor N-wollastonite. After oxidation, however, which gave only a slight increase of the oxygen content (Table 3), the oxygen-rich N-apatite was the only intergranular phase present in all materials. This can be explained if we consider that during treatments in nitrogen, such as hot-pressing, T4, and T9, the nitrogen content of the intergranular phase is increased, resulting in the formation of more nitrogen-rich phases.[12] Thus, it becomes obvious that material 8YH10SCp, that was hot-pressed at a higher temperature than 8Y, only contained the oxygen-poor (and nitrogen-rich) N-wollastonite as crystalline intergranular phase. During oxidation the nitrogen picked up during HP and T4 and T9 treatments is released and the oxygen-rich (and nitrogen-poor) N-apatite is formed. Since all crept materials contained the same crystalline intergranular phase—N-apatite—no effect on the creep resistance is expected. However, influences of the "initial" phase composition on the amount of primary creep cannot be excluded, but have not been the subject of this study.

The most striking result of the thermal treatments is a distinct grain growth. The mean grain size becomes larger the higher the temperature and the longer the duration of the treatment. This grain coarsening has to be taken into account to correctly explain experimental creep-rate data. The grain-size dependence of the steady-state creep rate is described by Eq. (1). In earlier studies performed in bending[13,14] a grain-size exponent m of unity was found for two hot-pressed silicon nitrides and Si_3N_4/SiC nanocomposites in the grain-size range of 0.12–1.3 μm. Grain-size exponents in the range of $m = 2.4$–3.1 were also reported in the literature.[15,16] In these studies, however, the materials were tested in compression and they contained large amounts of a glassy phase so that the deformation mechanism must be assumed to be different from that observed here. Furthermore, the range of grain sizes investigated in these two studies was very small.[15,16] Owing to the similarity of the materials of the present work and those studied in Refs. 13 and 14, and because of the less pronounced difference between bending and tension than between compression and tension, the grain-size exponent found in Refs. 13 and 14 was used for further calculations. Using $m = 1$ in Eq. (1), the steady-state creep rate obtained for materials of different grain size, d_m, can be normalised to a single standard grain size, $d_{corr.}$, by the relationship

$$\dot{\varepsilon}_{s,corr.} = \dot{\varepsilon}_s \cdot \frac{d_m}{d_{corr.}} = \dot{\varepsilon}_s \cdot GSR \tag{4}$$

where $\dot{\varepsilon}_{s,corr.}$ is the normalised creep rate, $\dot{\varepsilon}_s$ is the measured creep rate, and GSR is the grain-size ratio. Hence, normalisation is of the creep rate is achieved by multiplication with the grain-size ratio GSR, and the normalised creep-rate ratio is obtained by

$$CRR_{corr} = CRR \cdot GSR. \tag{5}$$

The grain-size ratios for the correction of CRR-T4 and CRR-T9 are given in Table 4 together with the $CRR_{corr.}$-values. These values describe the "real" effect of the thermal treatments, since the effect of grain growth has been compensated for. They are used to discuss the effect of SiC particles and heat treatments on the creep resistance.

From the creep rates of materials 8Y and 8YH10SCp, a value of $CRR_{corr.} = 0.60$ is obtained. In the case that the reduced oxygen content is responsible for the increased creep resistance, this value should be equal to CRR-$T4_{corr.}$ of material 8Y (0.65, Table 4), because materials 8YH10SCp and 8YT4 contain similar amounts of oxygen before and after the creep testing (Table 3): But, CRR-$T4_{corr.}$ is larger and accordingly the "real" effect of treatment T4 on the creep resistance of material 8Y is smaller than that of the addition of 10 wt.% SiC particles. Furthermore, the values of CRR-$T4_{corr.}$ and CRR-$T9_{corr.}$ for material 8YH10SCp are smaller than the corresponding values for material 8Y, indicating that the treatments in reducing atmosphere are more effective for the nanocomposite than for the monolithic Si_3N_4. So, it has to be concluded that the reduction of the oxygen content cannot be the only reason for the improved creep resistance.

TEM investigations of materials 8YT9 and 8YH 10SCpT9 revealed specific modifications of the microstructure. Figs. 8 and 9 are examples of TEM images, showing typical features of the microstructure of the heat-treated materials. In material 8YT9, epitaxial crystallisation of Si_3N_4 into multigrain junctions was found (see arrow in Fig. 8). This feature lead to an increase in

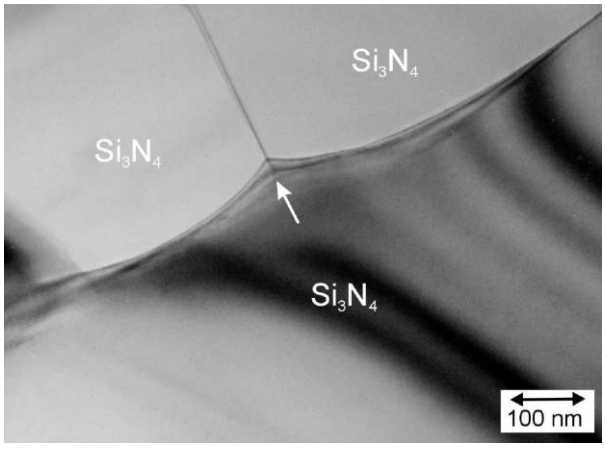

Fig. 8. TEM micrograph of material 8YT9 showing epitaxial crystallisation of Si_3N_4 into a multigrain junction (arrow) (courtesy H.-J. Kleebe).

the roughness of the grain boundary and, hence, to a hindrance of grain-boundary sliding. This phenomenon is thought to improve the creep resistance of the monolithic Si_3N_4. For material 8YH10SCpT9, on the other hand, a similar modification of the grain-boundary structure could be detected. Besides this finding, however, the formation of very irregular and interlocked grain boundaries was observed in the close vicinity of SiC particles, as shown in Fig. 9. Such tightly interlocked grain boundaries are expected to efficiently inhibit grain-boundary sliding and are thought to be responsible for the distinct improvement of the creep resistance of the nanocomposites.

Summarising the results obtained in this study, it is emphasised that the effects controlling the creep behaviour of heat-treated and particle-reinforced Si_3N_4 nanocomposites are quite complex. However, a schematic diagram may help to illustrate the various influences on the *microstructure*, the *grain-boundary chemistry* and the *micromechanics of creep*. Both the heat treatment in N_2 atmosphere and the addition of SiC particles modify the grain-boundary chemistry (arrows 1 and 2 in Fig. 10), leading to a reduction of the oxygen content of the material, c_O, and a variation of the activation energy for creep, Q_c. The change of the oxygen content affects the amount of the intergranular phase and causes the appearance of different crystalline phases which obviously reduce the creep rate (arrow 3). Additionally, heat treatments modify the *microstructure* by inducing grain growth (arrow 4), resulting in a reduced creep rate (arrow 5). The presence of SiC particles, on the other hand, influences the microstructure by effectively impeding grain growth and retaining a fine grain size (arrow 6 in Fig. 10), thereby giving rise to a high creep rate (arrow 5). In combination with a suitable heat treatment, the presence of the SiC particles results in the formation of markedly interlocked grain boundaries (arrow 7). Furthermore, small SiC particles located on two-grain

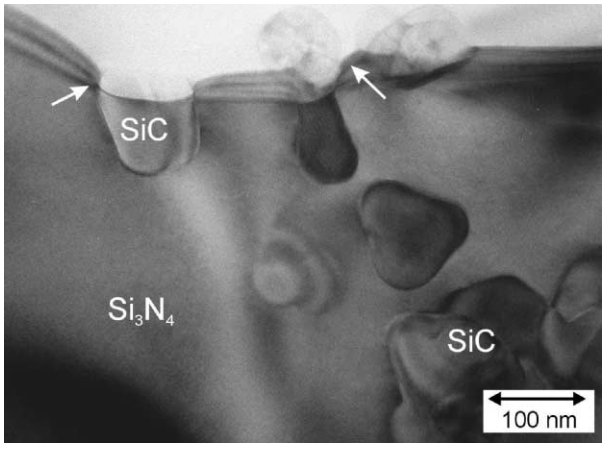

Fig. 9. TEM micrograph of material 8YH10SCpT9 showing the formation of a very rough and interlocked grain boundary (arrows) (courtesy H.-J. Kleebe).

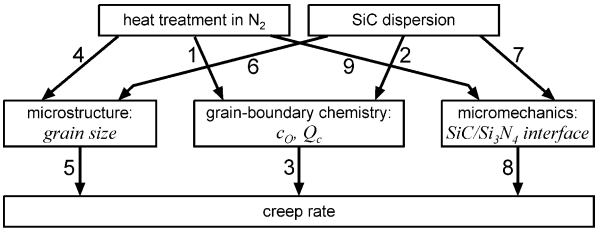

Fig. 10. Schematic of influences observed.

junctions directly influence the sliding behaviour of neighbouring grains by grain pinning (arrow 8) as has been suggested previously[2]. Both the change of the grain shape by epitaxial crystallisation of Si_3N_4 in multigrain junctions and the formation of interlocked grain boundaries largely affect the *micromechanical interaction* between Si_3N_4 grains (arrow 9), leading to an distinct improvement of the creep resistance (arrow 8).

Finally, it can be concluded that *chemical* and *microstructural* effects caused by heat treatments or a SiC dispersion result in a modification of the *micromechanical* behaviour of the matrix grains. Thus, for silicon nitride based ceramics the design of a microstructure with minimised capability of grain-boundary sliding is the key for the design of highly creep-resistant materials.

5. Summary

It was the aim of the present work to improve the understanding of the role of SiC particles during creep of Si_3N_4/SiC nanocomposites. For that, the microstructural development and the creep behavior of a submicron-sized silicon nitride material with and without the addition of a nanosized SiC particle dispersion was studied experimentally. Both reducing and oxidizing heat treatments were used to provoke effects that may be assumed to synergically intensify the influences of the SiC phase.

The action of SiC particles was found to consist of the simultaneous operation of chemical, microstructural, and micromechanical effects. The *chemical effect* of the SiC particles was identified to result in a reduction of the oxygen content of the Si_3N_4 matrix. The same effect was achieved when monolithic, SiC-free silicon nitride was heat-treated in a reducing environment. Once the reduction of the oxygen content had occurred, it could not be reversed by a subsequent oxidation treatment. The creep behaviour, however, was not much affected by this chemical effect.

Additionally, heat treatments in a reducing environment caused significant grain growth in monolithic Si_3N_4 to occur, whereas it was effectively restricted in the nanocomposite variants. Thus, a *microstructural effect* can be attributed to the SiC particles that consists

in a stabilisation of the grain structure. Increased grain size gave rise to decreased creep rates, as is to be expected. When normalized to equal grain size, however, the creep-rate reduction was more pronounced in the nanocomposites than in the monolithic material. This leads to the conclusion that a further influence of the SiC phase must be assumed.

TEM observations showed increased roughness and irregular shape of Si_3N_4 boundaries in SiC containing materials. As a consequence, the observed grain-boundary serrations are taken as the reason for a reduced capability for grain-boundary sliding. Thus, a *micromechanical effect* is ascribed to the SiC particles, too.

Acknowledgements

The authors thank Dr. M. Herrmann and Dr. H. Klemm of IKTS Dresden, Germany, for the support in materials preparation, thermal treatments, and measurement of the oxygen content. We are very grateful to Professor H.-J. Kleebe of Colorado School of Mines, Golden, CO, USA, for performing the TEM investigations. Financial support by the German Research Council (DFG) within the special research program "Micromechanics of multiphase materials"—SFB 371, project D2, is gratefully acknowledged.

References

1. Rendtel, A. and Hübner, H., Creep resistant silicon nitride ceramics–approaches of microstructural design. *Ceram. Eng. Sci. Proc.*, 2000, **21**(4), 515–526.
2. Niihara, K., New design concept of structural ceramics– ceramic nanocomposites. *J. Ceram. Soc. Jpn.*, 1991, **99**, 974–982.
3. Rendtel, A., Hübner, H., Herrmann, M. and Schubert, Ch., Si_3N_4/SiC nanocomposite materials: II, hot strength, creep, and oxidation resistance. *J. Am. Ceram. Soc.*, 1998, **81**, 1109–1120.
4. Zalite, I., Boden, G., Schubert, Ch., Lodzina, A., Plitmanis, J. and Miller, T., Sintering of fine silicon nitride powders. *Latv. Chem. J.*, 1992, **2**, 152–159.
5. Herrmann, M., Schubert, Ch., Rendtel, A. and Hübner, H., Si_3N_4/SiC nanocomposite materials: I, fabrication and mechanical properties at room temperature. *J. Am. Ceram. Soc.*, 1998, **81**, 1095–1108.
6. Rendtel, A. and Hübner, H., Precise tensile creep measurement with refractory ceramics. *cfi/Ber. DKG*, 2001, **78**(8), E45–E47.
7. Norton, F. H., The flow of ceramic bodies at elevated temperatures. *J. Am. Ceram. Soc.*, 1936, **19**, 129–134.
8. Rendtel, P., Rendtel, A., Hübner, H., Klemm, H. and Herrmann, M., Effect of long-term oxidation on creep and failure of Si_3N_4 and Si_3N_4/SiC nanocomposites. *J. Eur. Ceram. Soc.*, 1999, **19**, 217–226.
9. Klemm, H., Herrmann, M. and Schubert, C., High temperature oxidation of silicon nitride based ceramic materials. In *Proc. 6th Internat. Symp. on Ceram. Mater. & Comp. for Engines 19.-24.10.1997*, ed. K. Niihara, S. Kanzaki, K. Komeya, S. Hirano and K. Morinaga. Arita, Japan, 1997, pp. 75–84.
10. Ohji, T., Nakahira, A., Hirano, T. and Niihara, K., Tensile creep behaviour of alumina/silicon carbide nanocomposite. *J. Am. Ceram. Soc.*, 1994, **77**, 3259–3262.
11. Sternitzke, M., Review: Structural ceramic nanocomposites. *J. Eur. Ceram. Soc.*, 1997, **17**, 1–22.
12. Pullum, O. J. and Lewis, M. H., The effect of process atmosphere on the intergranular phase in silicon nitride ceramics. *J. Eur. Ceram. Soc.*, 1996, **16**, 1271–1275.
13. Acchar, W., Rendtel, A., Hübner, H. and Schubert, C., Improvements in the creep resistance of hot-pressed silicon nitride (HPSN). In *Engineering Ceramics, THIRD EURO-CERAMICS,* Vol. 3, ed. P. Duran and J. F. Fernandez. Faenza Editrice Iberica S.L, Madrid, Spain, 1993, pp. 405–410.
14. Rendtel, A. and Hübner, H., Creep behavior and lifetime of Si_3N_4/SiC nanocomposites. In *Advances in Ceramic-Matrix Composites III, Ceramic Transactions*, ed. N. P. Bansal and J. P. Singh. American Ceramic Society, Westerville, OH, USA, 1997, pp. 523–534.
15. Yoon, S.-Y., Kashimura, H., Akatsu, T., Tanabe, Y., Yamada, S. and Yasuda, E., Grain size dependency on the creep rate in hot-pressed silicon nitride. *J. Ceram. Soc. Jpn., Int. Ed.*, 1996, **104**, 935–941.
16. Zhan, G.-D., Mitomo, M., Ikuhara, Y. and Sakuma, T., Effects of microstructure on superplastic behavior and deformation mechanisms in β-silicon nitride ceramics. *J. Am. Ceram. Soc.*, 2000, **83**, 3179–3184.